Int. J. Electrochem. Sci., 10 **(2015)** 3914 - 3922

International Journal of
ELECTROCHEMICAL
SCIENCE
www.electrochemsci.org

Characteristics of Polymer-Fullerene Solar Cells with ZnS Nanoparticles

Kin-Tak Lam[1], *Yu-Jen Hsiao*[2], *Liang-Wen Ji*[3,*], *Te-Hua Fang*[4,*], *Wei-Shun Shih*[3], *Jun-Nan Lin*[3]

[1] Institute of Creative Industries Research, Fuzhou University, Fuzhou, Fujian 350108, P. R. China
[2] National Nano Device Laboratories, National Applied Research Laboratories, Tainan 741, Taiwan
[3] Institute of Electro-Optical and Materials Science, National Formosa University, Yunlin 632, Taiwan
[4] Department of Mechanical Engineering, National Kaohsiung University of Applied Sciences, Kaohsiung 807,Taiwan
[*]E-mail: lwji@seed.net.tw; fang.tehua@msa.hinet.net

Received: 27 January 2015 / *Accepted:* 2 March 2015 / *Published:* 23 March 2015

The efficiency of the organic conjugated polymer solar cells can be significantly improved when we use organic conjugated polymers and fullerene blends as the photoactive layers of the cells. In this paper, the authors demonstrate the preparation and characteristics of polymer-fullerene solar cells based on ZnS nanoparticles (NPs) of composite films. With blending ZnS NPs in the polymer-fullerene matrix, it was found that efficiencies of the solar cells with 0, 15, 30 and 45 wt% ZnS NPs were 2.03, 2.18, 1.16 and 0.78 %, respectively, and the external quantum efficiency (EQE) of the solar cells was maximum while the concentration of the ZnS NPs reached 15 wt%. It was also found that the ZnS NPs can increase exciton generation and electron carrier transport under some experimental condition, and will improve the open circuit voltage of the polymer-fullerene solar cells.

Keywords: heterojunction; polymer-fullerene solar cell; ZnS nanoparticles

1. INTRODUCTION

Due to the aqueous solution process in the manufacturing process is relatively simple, the organic conjugated polymer solar cell as a potential of the organic photovoltaic devices being active research. This technique for manufacturing of the solar cell, there is a lower cost and higher productivity [1].

Polymer or hybrid solar cells often utilize a nanostructured interpenetrating network of electron-donor and electron-acceptor materials [2-6]. In other words, the hybrid polymer solar cells using blends of the conjugated polymer and inorganic materials to convert sunlight into electric

charges [4-6]. Moreover, it can be expected that such a devices will integrate the advantages of two materials, i.e., (1) high electron mobility of inorganic semiconductors and photosensitivity, and (2) high hole mobility of conjugated polymers [7]. However, currently the power conversion efficiency (PCE, η) of the hybrid photovoltaic devices is still very low due to the poor interfacial junction between the organic and inorganic materials. Thus, many researchers are aimed at improving the heterojunction between two materials [7-10]. In these studies, an important method is to use two materials having complementary operation of the *p*-type and *n*-type electronic properties for the hybrid polymer solar cell [11-14]. Accordingly, we use organic conjugated polymers and fullerene blends the formation of electron donor/acceptor heterojunction structure, i.e., P3HT poly [(3-hexylthiophen e-2,5-diyl)] and C_{60} derivative PCBM [(6,6)-phenyl-C61-butyric acid methyl ester] material with the blending ZnS nanoparticles (NPs) on polymer-fullerene matrix, so the efficiency of our organic conjugated polymer solar cell is significantly improved. Among these structure, inorganic semiconductor ZnS was used as the *n*-type material in combination with the P3HT: PCBM photoactive layer. This property makes P3HT: PCBM photoactive layer very attractive as an absorber in hybrid polymer solar cells. In this study, we focused on adjust the concentration of ZnS using chemical bath deposition method on P3HT: PCBM photoactive layer. The P3HT: PCBM heterojunctions with the blending ZnS NPs on polymer-fullerene matrix has been made to study the light absorption characteristic and investigate their photovoltaic properties for the first time.

2. EXPERIMENTS

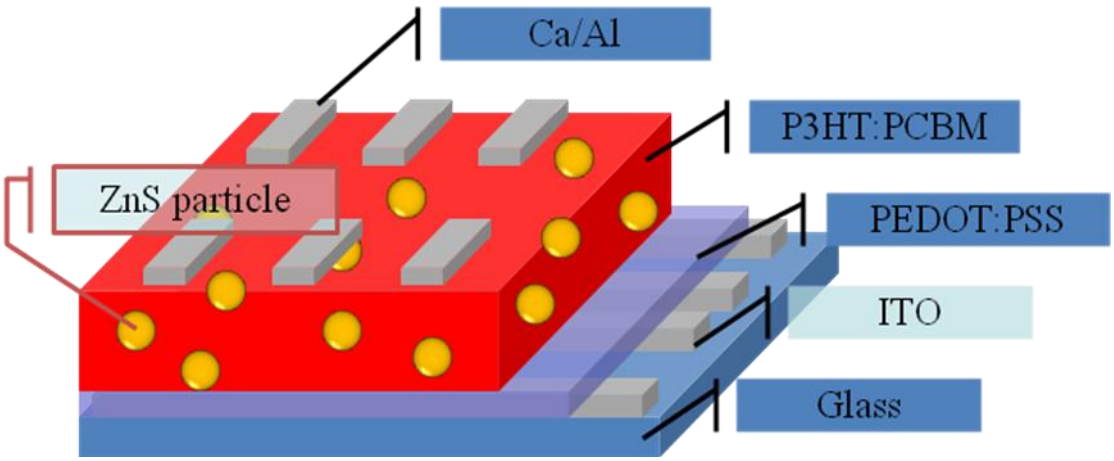

Figure 1. Device structure consists of an active layer of P3HT: PCBM: ZnS NP sandwiched between Ca/Al electrode and conducting electrode of PEDOT: PSS on ITO glass substrate.

A configuration was employed for the electrical studies of polymer-fullerene solar cell. The electrical conductivities measurements were done using the configuration presented in Figure 1. Polymer-fullerene solar cells were prepared by spin coating a precursor solution of P3HT: PCBM: ZnS NP layer on pre-cleaned ITO (tin-doped indium oxide) glass substrates. The indium tin oxide (ITO)

glass substrates with a sheet resistance of 10 Ω/sq were first cleaned with detergent, then, ultrasonicated in deionized water, acetone and isopropanol, and subsequently dried in oven. A transparent bilayer electrode comprising PEDOT:PSS as hole collection was spin-coated onto the ITO substrate at 2600 rpm for 60 s and then dried at 120 °C for 30 min. The P3HT:PCBM photoactive layer was first fabricated by spin-coating P3HT: PCBM with 1:0.8 weight ratio solution in chlorobenzene onto the PEDOT: PSS layer in a nitrogen-filled glove box. Then, the nanocrystalline ZnS (nc-ZnS) was doped in P3HT: PCBM solution in chlorobenzene with variable weight ratios (0, 15, 30 and 45 wt%). In this study, the ZnS NPs (purities > 99.9%) was prepared by the chemical bath deposition method using $ZnSO_4$, thiourea ($(NH_2)_2CS$) and ammonia. In a typical procedure, 0.1 M $ZnSO_4$ and 0.5 M $(NH_2)_2CS$ was put into a 100 mL beaker and dissolved with 15 mL NH_3 under vigorous magnetic stirring at 80 ^oC temperature for 30 min. To fabricate the nc-ZnS-doped active layer, P3HT: PCBM: ZnS NP solution was spin-coated onto the PEDOT:PSS layer at a spin-coating speed of 1500 rpm for 60 s and annealed temperature at 120 °C for 10 min. The ratios of P3HT: PCBM: ZnS NP were 1:0.8, 1:0.8:0.15, 1:0.8:0.3 and 1:0.8:0.45, respectively. Finally, Ca/Al was deposited on the top of polymer-fullerene solar cell by a thermal evaporator as an electrode. The film thicknesses of P3HT: PCBM: ZnS NP, PEDOT:PSS, Ca and Al were about 180, 85, 25 and 100 nm, respectively. The active area of the device was estimated to be 0.04 cm^2.

The morphology and microstructure were examined by Cryo-Transmission Electron Microscope (Cryo-TEM) operating at an accelerating voltage of 100 keV. The absorption spectra of hybrid active layers were measured at room temperature using a Hitachi U-3310 ultraviolet-visible (UV-Vis) spectrophotometer. Device current-voltage measurements (Keithley 2410 source meter) of solar cell were obtained by using a solar simulator with an AM 1.5 filter under an irradiation intensity of 100 mW cm^{-2}. The external quantum efficiency (EQE) measurements were performed by an Xe lamp in combination with a monochromator and filters.

3. RESULTS AND DISCUSSION

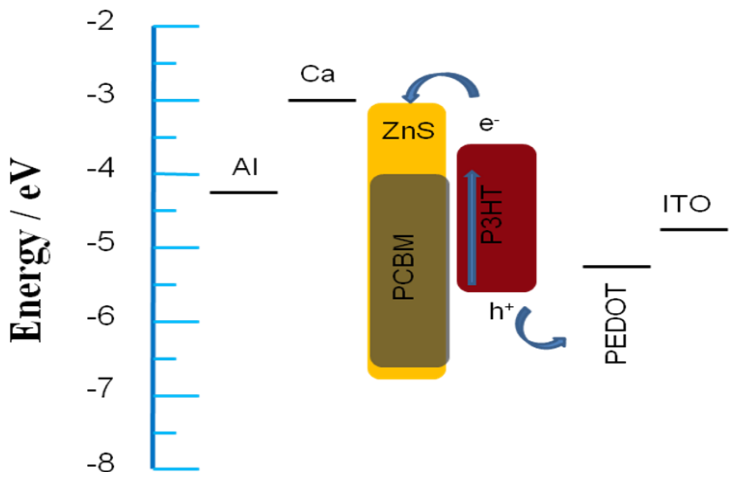

Figure 2. Schematic energy level diagrams for the device, with energy level in eV relative to vacuum.

Among numerous photoactive donor/acceptor composites, the p-type conjugated polymers with fullerene derivatives like P3HT/PCBM blend has been intensively investigated recently. The active layer of bulk heterojuction solar cell constructed by blending p-type conjugated polymers with n-type conjugated polymers, fullerenes, fullerene derivatives or nanoparticles [15-16]. The charge carrier mobility of the polymer and fullerene blend are comparatively low, the short exciton diffusion length in the active layer and weak absorbance, the solar energy conversion efficiencies of the devices are limited. To solve this problem, other materials are presented in order to improve electron transport and absorbance, such as CdS/P3HT photoactive heterojuction [17]. Bredol et al. proposed a new hybrid bulk heterojunction photovoltaic system by mixing P3HT and ZnS [18]. It is successful synthesis of NPs-polymer hybrid solar cells show both advantages of semiconductor and very high open circuit voltage. The band gap of quantum dot crystal is size dependent and can be tuned. In this study, the novelty of P3HT/PCBM/ZnS blend with appropriate concentration provided formation of percolation pathways and improved power conversion efficiency (PCE).

Figure 2 presents the energy level diagram of P3HT: PCBM devices incorporating the P3HT: ZnS NP interfacial layer used in this study. This figure shows the highest occupied molecular orbital (HOMO) and lowest unoccupied molecular orbital (LUMO) levels of the P3HT: PCBM relative to vacuum level. The high conduction band and ideal valence band edge of P3HT: ZnS NP makes it an appropriate hole selective interfacial layer for the P3HT: PCBM photoactive layer. The free charges can diffuse in their individual component materials. In our device configuration, the P3HT: PCBM and P3HT: ZnS NP form a donor-acceptor heterojunction of the photogenerated excitons, P3HT: ZnS NP acts as electron transporting and hole blocking layer, and PEDOT: PSS acts as the hole transporting layer. Therefore the photogenerated electrons are transported to the Ca-Al contact via the ZnS NP (-3 eV) and the holes are transported through the HOMO of PCBM (-6.1 eV) and PEDOT (-5.2 eV) as shown in the diagram. It was found that the conduction band edge of ZnS nanoparticles under quantum confinement conditions was shifted to -3.5 eV, which is good for electrons collected by electrode.

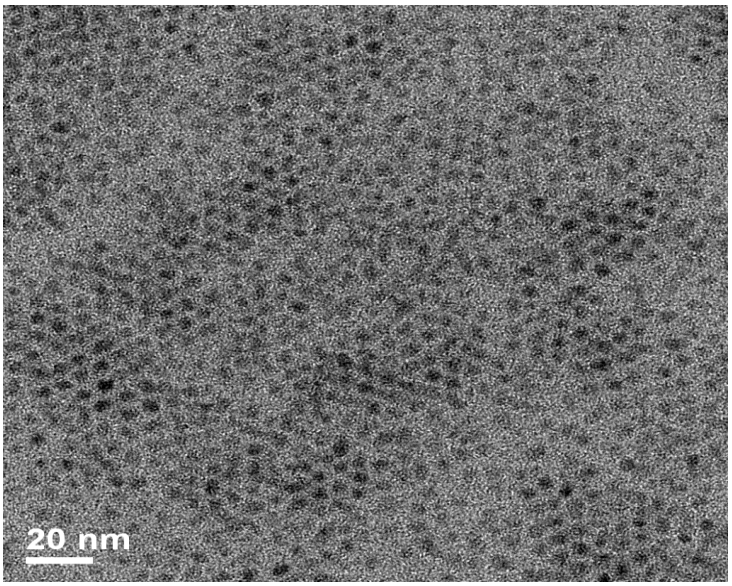

A

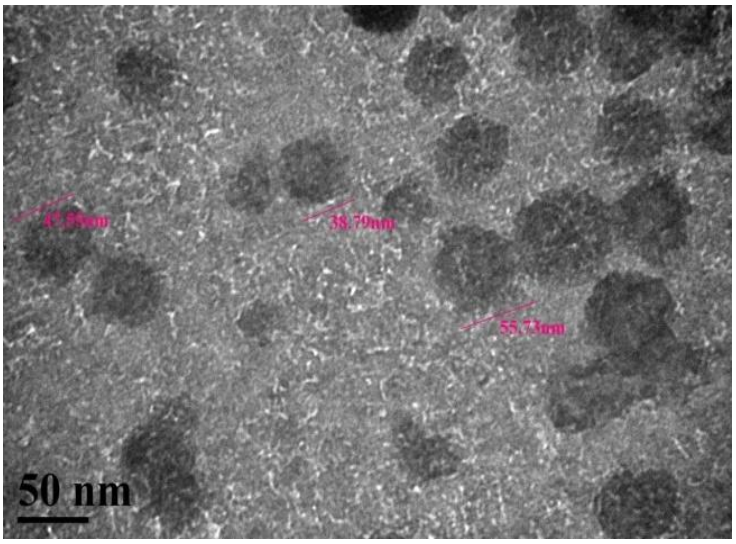

B

Figure 3. (a) The TEM image of ZnS nanoparticles and (b) P3HT: PCBM: ZnS NP hybrid film.

TEM analysis of the crystal ZnS NPs provided further insight into the nanostructural properties. The spherical morphology was clearly observed, as evidenced from TEM images at figure 3(a), and possessed a uniform dispersion with the average diameter of the ZnS NPs about 5 nm. To investigate the distribution of ZnS NPs in photoactive layer, we characterized the microstructures of the P3HT: PCBM: ZnS NP photoactive films by TEM. Figure 3 (b) shows the TEM image of P3HT/ ZnS NP hybrid film. It was found that the nc-ZnS were dispersed well and the average diameter was about 45 nm. The nanocrystals were condensed by NPs. It was conjectured that the assemble effect arising from nanoparticles, are responsible for the decreasing of surface energy.

Erb *et al*. [19] and Kim *et al*. [20] have reported enhancement in PL of P3HT in blend films, indicating the reduction of the interface area between the polymer and PCBM where the PL quenching occurs. The PL quenching gives the evidence for exciton separation, thus PL quenching is important to obtain efficient hybrid solar cell. However, this does not mean that the higher PL intensity will gain the better efficiency of solar cell.

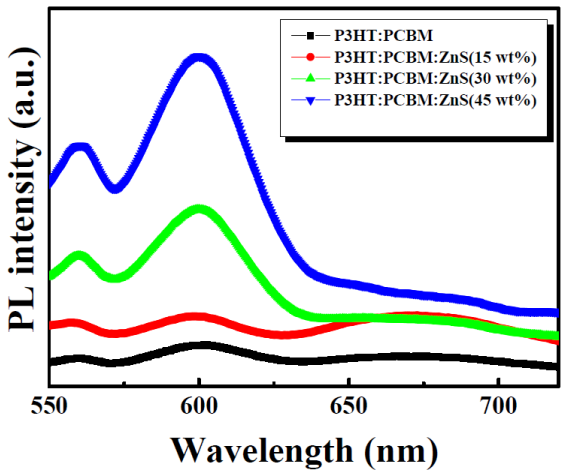

Figure 4. Current density-voltage (*J-V*) characteristic of P3HT: PCBM: ZnS NP solar cells for different ZnS NP ratio.

Figure 4 shows the PL spectra of P3HT: PCBM: ZnS NP films fabricated by spin-coating for different ZnS NP ratios, such as 0, 15, 30 and 45 wt%. It was observed that ZnS NP tend to increase PL intensity in the visible wavelength ranging from 550 to 650 nm, owing to non-radiative quenching pathways in the P3HT:PCBM material were be reduced. Due to the ZnS NP aggregation and the defacts of nanoparticles led to coarser phase segregation, adding ZnS NPs does not led to better PL quenching. On the other hand, formerly the responsible for the PL intensities, we thought that the ZnS NP aggregation can increase the recombination of exitons. It is expected that the high value of the light absorption intensity could lead to an improvement in the generation rate of excitons.

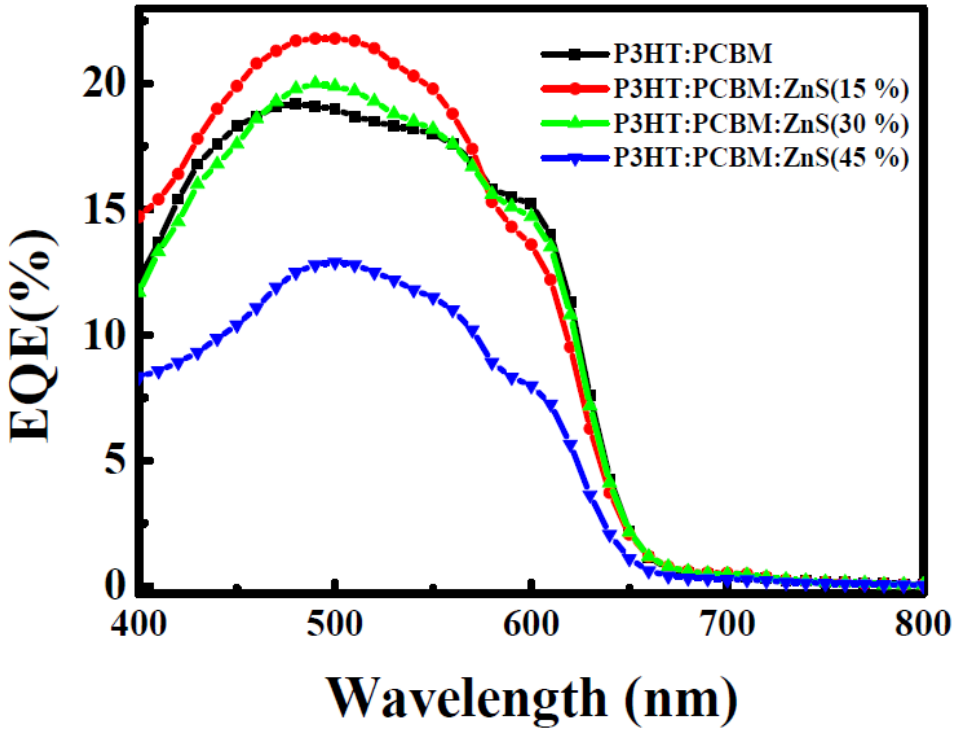

Figure 5. External quantum efficiency (EQE) spectrum of The ITO/PEDOT: PSS/P3HT: PCBM: ZnS NPs /Ca/Al devices for different ZnS NP ratio.

Figure 5 shows the External Quantum Efficiencies (EQE) values of the P3HT: PCBM: ZnS NP photoactive layers dissolved with various ZnS NP ratios, such as 0, 15, 30 and 45 wt%, under illumination from 400 to 800 nm. It was observed that the ZnS NP ratios would affect the EQE spectrum of the photovoltaic device. With a 500 nm illumination, we found that the maximum EQE values of the fabricated hybrid solar cells with 0, 15, 30 and 45 wt% ZnS NPs were 19, 22, 20 and 13 %, respectively. An EQE value for the P3HT: PCBM photoactive film using 15 wt% ZnS NP comparable to P3HT: PCBM: ZnS NP photoactive film that not only enhanced the charge generation ($\lambda < 650$ nm), but also improve the collection efficiency. The EQE magnitude is first slightly reduced from 22 to 20 % (ZnS NP = 30 wt%), followed by rapid decrease to 13 % (ZnS NP = 45 wt%). From this result, we conjecture that the EQE values may be related to the crystalline property as well as the surface morphology of the photoactive layer.

Fig. 6 shows the current density *versus* voltage (*J-V*) characteristic curves of the finished polymer-fullerene solar cells were measured under a simulated AM 1.5 illumination intensity of 100 mW/cm^2, and device parameters of the short-circuit current density (J_{sc}), the open-circuit voltage (V_{oc}), the fill factor (*FF*), and the power conversion efficiency (PCE, η) values of the P3HT: PCBM: ZnS NP photoactive layers prepared from the various ZnS NP ratios, such as 0, 15, 30 and 45 wt%. The PCE and fill factor *FF* were evaluated by the following relations:

$$\eta = \frac{J_m \times V_m}{P_{inc}} \quad (1)$$

$$FF = \frac{J_m \times V_m}{J_{sc} \times V_{oc}} \quad (2)$$

where P_{inc} is the incident light power. J_m and V_m represent the maximum current density and voltage, respectively. The J_{sc}, V_{oc}, *FF* and PCE values of the P3HT: PCBM: ZnS NP photoactive layers prepared from the various ZnS NP ratios are summarized in Table 1.

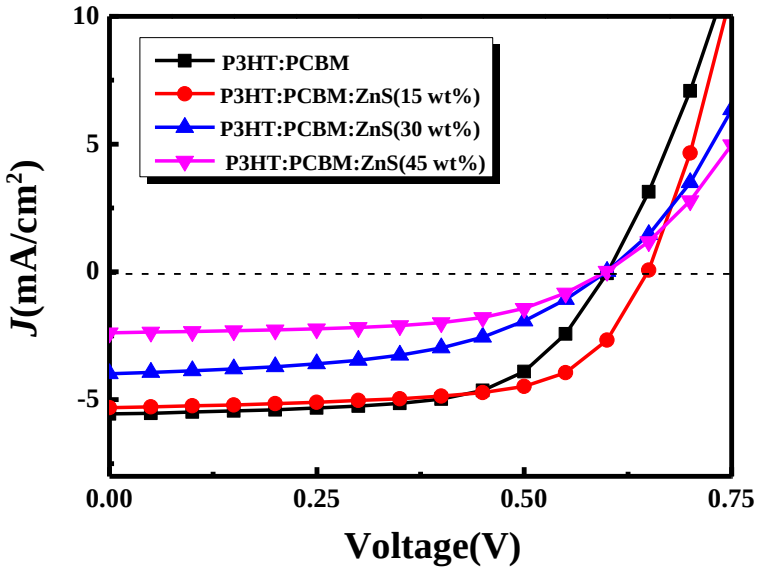

Figure 6. Current density-voltage (*J-V*) characteristic of P3HT: PCBM: ZnS NP solar cells for different ZnS NP ratio.

Table 1. Characteristics of the hybrid polymer solar cells for different ZnS NP ratio under illumination of AM 1.5 simulated solar light.

SCs with different ZnS NP ratio	J_{SC} (mA/cm^2)	V_{OC} (V)	R_S (Ω)	F.F. (%)	Efficiency
P3HT: PCBM	5.4	0.6	496	62	2.03
P3HT: PCBM: ZnS (15 wt %)	5.17	0.65	183	65	2.18
P3HT: PCBM: ZnS (30 wt %)	3.88	0.6	747	50	1.16
P3HT: PCBM: ZnS (45 wt %)	2.32	0.6	970	56	0.78

We can found that the J_{sc}, V_{oc}, *FF* and PCE values of the hybrid bulk heterojunction solar cell with 15 wt% ZnS NPs are superior to that heterojunction solar cell without ZnS NPs. The J_{sc}, V_{oc} and *FF* values of the hybrid bulk heterojunction solar cell increased from 5.4 to 5.17 mA/cm^2, 0.6 to 0.65 V and 62 to 65 %, respectively, while concentration of the ZnS NP reached from 0 to 15 wt% when P3HT: PCBM ratio was 1:0.8. While the former is smaller than the later by series resistance (R_s) comparison (R_s:183/496 Ω). It was observed that the power conversion efficiencies PCE η of hybrid bulk heterojunction solar cells with 0 and 15 wt% ZnS nanoparticles were 2.03 to 2.18 %, respectively. Using less than 15 wt% ZnS nanoparticles led to decrease a small degree of J_{sc}, which can be compensated by the increased voltage. At between 30 wt% and 45 wt% ZnS NPs, the V_{oc} is not sensitive to the P3HT: PCBM: ZnS NP ratio. Upon increasing more than 15 wt% ZnS Nanoparticles, the J_{sc} and PCE η continuously decreased, due to increasing the series resistance. In addition, more ZnS nanoparticles afford more phase segregation; this effect is counteracted by a higher J_{sc}.

From our experiments, it may be concluded that the observed improvement in the electrical properties of the P3HT: PCBM photoactive layer dissolved with the ZnS nanoparticles is caused by a favorable change in the enhanced crystallinity, and the absorption light intensity of the photoactive layer due to the high vapor density and low solubility of the mixing solvents. This result could be attributed to the ZnS nanoparticles can be used to grow an interpenetrating network in P3HT: PCBM photoactive layer.

4. CONCLUSIONS

In summary, we report that the optical, morphological and electrical properties of the P3HT: PCBM photoactive layer of polymer-fullerene solar cells can be significantly affected by the blending ZnS NPs on polymer-fullerene matrix. organic conjugated polymer solar cells with an ITO/PEDOT: PSS/P3HT: PCBM: ZnS NP/Ca/Al structure consisting of a P3HT: ZnS NP electron donor and a P3HT: PCBM acceptor in the photovoltaic active layer were fabricated. The short-circuit current density (J_{sc}), open-circuit voltage (V_{oc}), and fill factor (*FF*) were found to be 5.17 mA/cm^2, 0.65 V and 65 %, respectively for the P3HT: PCBM photoactive layer dissolved with 15 wt% ZnS nanoparticles when P3HT: PCBM ratio was 1: 0.8; the power conversion efficiency (PCE) was calculated to be 2.18 %. It may be concluded that the improved electrical parameters for the polymer-fullerene solar cells originate from the rough film surface, the high absorption intensity, as well as the good crystalline property of the photoactive layer.

ACKNOWLEDGEMENTS
This work was financially supported by National Science Council of Taiwan under contract number NSC-98-2221-E-150-005-MY3, NSC-100-2622-E-150-008-CC3 and NSC 101-2221-E-150-045.

References

1. K. Takanezawa, K. Hirota, Q.S. Wei, K. Tajima and K. Hashimoto, *J. Phys. Chem. C*, 111 (2007) 7218.

2. G. Yu, J. Gao, J.C. Hummelen, F. Wudl and A.J. Heeger, *Science* 270 (1995) 1789.
3. J.J.M. Halls, C.A. Walsh, N.C. Greenham, E.A. Marseglia, R.H. Friend, S.C. Moratti and A.B. Holmes, *Nature* 376 (1995) 498.
4. L.W. Ji, W.S. Shih, T.H. Fang, C.Z. Wu, S.M. Peng and T.H. Meen, *J. Mater. Sci.*, 45 (2010) 3266.
5. W.J.E Beek, M.M. Wienk and R.A.J. Janssen, *J. Mater. Chem*. 15 (2005) 2985.
6. W.J.E Beek, M.M. Wienk and R.A.J. Janssen, *Adv. Funct. Mater*. 16 (2006) 1112.
7. N. Kudo, S. Honda, Y. Shimazaki, H. Ohkita, S. Ito and H. Benten, *Appl. Phys. Lett*. 90 (2007) 183513-1.
8. W.U. Huynh, J.J. Dittmer, A.P. Alivisatos, *Science* 295 (2002) 2425.
9. K.M. Coakley and M.D. McGehee, *Appl. Phys. Lett.* 83 (2003) 3380.
10. C.Y. Jiang, X.W. Sun, G.Q. Lo, D.L. Kwong and J.X. Wang, *Appl. Phys. Lett*. 90 (2007) 263501-1.
11. B. O'Regan and M. Gra¨tzel, *Nature* 353 (1991) 737.
12. G. Yu and A.J. Heeger, *J. Appl. Phys*. 78 (1995) 4510.
13. R. Kersting, U. Lemmer, M. Deussen, H.J. Bakker, R.F. Mahrt, H. Kurz, V.I. Arkhipov, H. Bassler and E.O. Gobel, *Phys. Rev. Lett*. 73 (1994) 1440.
14. S. Barth and H. Ba¨ssler, *Phys. Rev. Lett.* 79 (1997) 4445.
15. Z.W. Chiu, Y.J. Hsiao, T.H. Fang, L.W. Ji, *Int. J. Electrochem. Sci.*, 10 (2014) 2391.
16. S.C. Chang, Y.J. Hsiao and T.S. Li, *Int. J. Electrochem. Sci.*, 10 (2015) 1658.
17. Y.C. Ing, Z. Zainal, A. Kassim, W. M. M. Yunus, *Int. J. Electrochem. Sci.*, 6 (2011) 2898.
18. M. Bredol, K. Matras, A. Szatkowski, J. Sanetra, A. Prodi-Schwab, *Sol. Energy Mater. Sol. Cells* 93 (2009) 662.
19. T. Erb, U. Zhokhavets, G. Gobsch, B. Raleva and P. Stuhn, *Adv. Funct. Mater.* 15 (2005) 1193.
20. Y. Kim, S. Cook, S.M. Tuladhar, S.A. Choulis, J. Nelson and M. Ree, *Nat. Mater.* 5 (2006) 197.